Received: 25 August 2020 | Revised: 7 December 2020 | Accepted: 17 January 2021

DOI: 10.1002/we.2620

RESEARCH ARTICLE

WILEY

A systematic evaluation of wind's capacity credit in the Western United States

Jennie Jorgenson | **Sarah Awara** | **Gord Stephen** | **Trieu Mai**

National Renewable Energy Laboratory
Golden, Denver, Colorado, USA

Correspondence
Jennie Jorgenson, 15013 Denver W Pkwy, Golden CO, 80401, USA.
Email: jennie.jorgenson@nrel.gov

Funding information
Wind Energy Technologies Office in the Department of Energy: Grant/Award Number: DE-AC36-08GO28308

Abstract

The degree to which wind energy can contribute to the capacity needed to meet resource adequacy requirements, also known as capacity credit (CC), can be impacted by many factors. The CC varies regionally with wind resource and correlation to net load and may also vary with wind technology (land-based versus offshore) and turbine specifications. We use a probabilistic resource adequacy tool to systematically assess the CC of multiple technologies for near-term wind deployment across the Western US power system to help inform planning decisions. We find that wind CC varies by weather year and location but averages 16% for land-based turbines and 41% for offshore turbines, with large regional variations. The average wind CC increases to 20% for land-based and 53% for offshore when considering only the sites in the top 25th percentile of capacity factor. The CC of land-based wind is generally lower than its capacity factor, which indicates a low correlation of generation to system needs. However, offshore wind shows a substantially higher CC, which is driven by not only a higher capacity factor but also a greater correlation with system needs.

KEYWORDS

capacity credit, offshore wind, probabilistic analysis, resource adequacy, wind energy

1 | INTRODUCTION

As the deployment of wind generation increases, questions arise about maintaining the existing level of supply security with variable sources of generation. Assessments of system adequacy and security can help determine the reliability of a power system.[1] A power system is adequate if the supply can meet the demand and is secure if it can adequately respond to disturbances on the system.[1] The percentage capacity contribution of a specific resource to the overall system adequacy is also called the resource's capacity credit (CC). The terms CC and capacity value (CV) have been used interchangeably in the literature. However, we follow an established convention to refer only to physical capacity (CC) rather than monetary or economic CV in this paper.[2] Two main methods are used to estimate CC: reliability-based and approximation-based methods.[3] Reliability-based methods typically use models to calculate reliability metrics such as the loss of load probability (LOLP, measured as a percentage), loss of load expectation (LOLE, given as a number of hours with expected shortage), or expected unserved energy (EUE, with a magnitude measured in units of MWh or GWh) given inputs including hourly loads and generator data.[4] A reliability-based method calculates the CC of an incremental resource by computing the reliability metric (e.g., LOLP, LOLE, or EUE) before and after the addition of the new resource. Any change in the reliability metric can then be attributed to the incremental resource. Approximation-based methods, which are simpler, usually calculate the

CC of a unit based on the capacity factor (CF) (or the percentage output of a plant relative to its nameplate capacity) during a predetermined period, generally the hours where the system is expected to be under stress. The system can be under stress during hours of peak load or unexpected generator outages. CF-based approximations typically do not consider as many aspects of system operation as reliability-based methods, and they can miss certain factors (e.g., transmission congestion, the impact of incremental resources on shifting or impacting the highest risk periods, and intertemporal constraints on energy-limited resources) that are important to consider when evaluating CC.[5,6] Thus, reliability-based resource adequacy (RA) methods are recommended whenever data and computation capabilities are available. [7,5]

Researchers have been studying the CC of renewable energy for decades, using many methods.[8–9,7,6,10–11] The IEEE Task Force on the CV of Wind Power summarizes the methods currently in use, suggests a recommended method, and lists some of the gaps in the literature.[7] Previous research suggests that many factors influence the CC of wind, including the share of installed wind capacity on the system, the method used to calculate CC, the underlying wind resource, and the number of years of weather data used.[12–16,10,17–19] A review paper finds that the CC of wind is often close to its average CF (25%–40%) when the share of wind power is small, but increasing the share of wind decreases the CC, especially in smaller systems.[10] An evaluation of the Western US power system shows a lower land-based wind CC of 5%–30% depending on the region.[20] Research on the Irish system finds that the average CC of 1000 MW of wind is around 28% but falls to 14% for 4000 MW for a system with around a 5000-MW peak demand.[15] On the Spanish system, wind exhibits a CC of 20%–30% and decreases with wind penetration, but the rate of decline with penetration seems to be lower than the rate for solar technologies.[19] An analysis of the Australian system shows wind yields a CC of 7%–24% but much lower (7%–9%) in the long run with continued wind deployment.[17] Some studies have also begun to estimate the CC associated with offshore wind energy, including two studies of the Northeastern United States, showing CCs of 15%–35%.[21,13]

The RA contribution of renewable energy (often quantified by the CC) can have a direct impact on deployment. Utilities and load-serving entities need dependable capacity to replace retiring generator capacity or to keep up with load growth, which requires an understanding of the RA characteristics of these technologies. Established capacity markets provide economic incentives for the provision of firm capacity, requiring accurate estimates of renewable CC. Even without capacity markets, CC estimates are needed for capacity expansion models or utility resource planning processes. Despite this need, a rigorous high geographic resolution assessment for CC does not yet exist, as it does for other value metrics such as levelized cost of electricity.[22,23] In this analysis, we begin to fill the gap using a systematic approach to account for technology (i.e., land-based versus offshore) and turbine specifications to find a geographically resolved estimate of the marginal CC of wind. Our approach is unique considering not only the broad geographic resolution we evaluate, which can provide insight beyond its footprint due to the diversity in terrain, but also due to the consideration of transmission interconnections between regions, which only a limited number of studies consider.

2 | METHODOLOGY AND ASSUMPTIONS

We calculate the marginal CC systematically for 10,113 geographical sites covering the US portion of the Western Interconnection with a 20-km by 20-km resolution. We assess all sites to get a comprehensive set of wind CC estimates; however, we recognize that many factors influence the suitability of any given site for wind deployment, including costs, siting restrictions, energy production, and system needs.[24] In other words, we do not evaluate the full economic potential of all sites but only one component influencing deployment potential by employing a probabilistic reliability-based approach to estimate CC. This section describes the methodology, assumptions, and the data for our analysis.

2.1 | RA assessment model

Probabilistic RA tools quantify the risk of being unable to serve demand at all times with metrics such as LOLE, LOLP, EUE, or normalized expected unserved energy (NEUE), which is the total EUE, typically measured in MWh or GWh, divided by the total load (also in MWh or GWh) often reported in terms of parts per million (ppm). There are two general approaches for calculating these metrics: analytical (also referred to as Capacity Outage Probability Calculations or convolution methods) and simulation-based (i.e., Monte Carlo).[4]These tools analyze the distribution of possible system states given the probability of generator and transmission outages, generation from variable generation resources such as solar and wind, and demand. RA models assess a large number of possible system states and calculate probabilistic reliability metrics such as LOLE or EUE. RA tools provide a more robust approach to calculating reliability than approximation-based (e.g., CF-based) methods such as planning reserve margin metrics.

For this analysis of wind CC, we apply the National Renewable Energy Laboratory's (NREL's) Probabilistic Resource Adequacy Suite (PRAS) tool.[25] It uses Monte Carlo samples from probability distributions for generator availability and interregional power transfer constraints to calculate the loss of load due to supply shortfall or power transfer constraints.[21,26–27] Specifically, for each hour, we use 100,000 Monte Carlo draws of forced generator outages to compute the LOLE and EUE for a given level of net load (determined by the hourly demand less any contribution from weather-dependent resources such as wind and solar), which are aggregated into annual values. We compute these metrics before and after an incremental amount of wind capacity is added and attribute the reduction of LOLE or EUE to the wind, which can then be used to determine the CC of the marginal wind capacity.

2.2 | Base case system

A full RA assessment of large power systems requires extensive data for generator characteristics, transmission topology, and time series profiles such as load. We use data derived from previous analysis of the US Western Interconnection, with balancing authority (BA) areas shown in Figure 1.[28,27] This region is useful to study due to its substantial size, encompassing diverse terrain and wind resources which makes it more generally applicable. In addition, the Western United States, like much of the world, has seen increased deployment of wind energy which will likely continue.[28,29] We use publicly available data to match the 2017 generator fleet which is modeled as shown in Table 1, including existing wind, utility-scale solar photovoltaics (PV), and concentrating solar power (CSP).[30] The installed capacity of distributed PV per BA is not available publicly. Therefore, we determine BA-level distributed PV levels by applying county-level data,[31] disaggregating by population level with a gridded population data set, and then summing to each BA.[32] The hourly profiles for existing wind, utility-scale PV, distributed PV, and CSP are from the Wind Integration National Dataset (WIND) Toolkit[33] and the National Solar Radiation Database,[32] processed through NREL's System Advisor

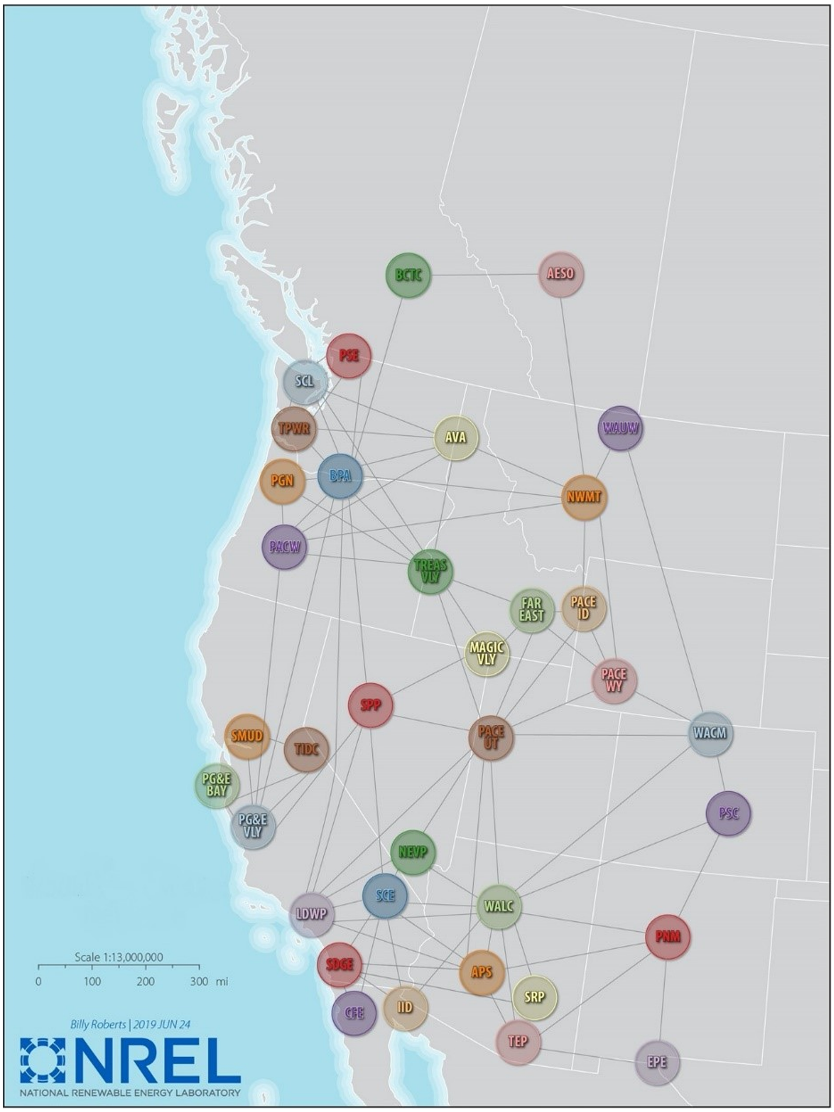

FIGURE 1 Balancing authority (BA) regions for the Western US footprint.[37] We consider interregional power transfer limits between the BA regions mapped here but no intraregional constraints within BAs. Note that offshore wind sites are assigned to the nearest neighboring BA

Model[34] with specific technology assumptions to generate CF profiles.[35] We adapted BA-level hourly load from the North American Renewable Integration Study, which collected load profiles from independent system operators, regional transmission organizations, and Federal Energy Regulatory Commission data, shown in Table 1.[36] We employ 7 years of system load, wind, and solar profiles (2007 through 2013). The total average wind generation as a fraction of total load is 8.4% for the seven weather years considered and 4.9% for PV. We use multiple years of weather data to capture the impact of interannual variability, as is recommended for a robust analysis of CC.[7,5,10]

2.3 | Calculating CC

We start with the base system described in the previous section to systematically estimate the marginal CC of all wind sites using a gridded dataset covering the entire Western United States in 20-km by 20-km grid cells.[33] NREL's WIND Toolkit contains wind data for 2-km by 2-km grid cells for the footprint studied here. However, to reduce computational demands and to match the footprint of modern wind power plants more closely, we aggregated profiles to a resolution of 20 km by 20 km. We consider three turbine types: two technologies for land-based sites and one for offshore sites. We generate hourly wind CF profiles for the gridded dataset, creating 7859 onshore (land-based) and 2254 offshore grid cells, which represents the full footprint covered by the WIND Toolkit, capturing the Outer Continental Shelf up to 200 nautical miles from the shoreline. Table 2 shows the technology specifications we use to generate the profiles for the incremental wind, with corresponding power curves shown in the appendix (Figure A1). The two land-based technology specifications are characteristic of turbines that are available in the United States today (denoted "*current* technology") and turbines from a "*future* technology" category that extends recent trends toward larger

TABLE 1 Assumptions for the exsting generating capacity by type, along with system demand

Generating capacity by type[a]	
Wind	23,00 MW
Utility-scale PV	15,200 MW
Distributed PV	9580 MW
CSP	1870 MW
Hydropower	65,400 MW
Coal	27,300 MW
Natural gas	64,200 MW
Nuclear	7430 MW
Other[b]	9520 MW
Demand characteristics	
Peak hourly load	159,000 (7-year range: 152,000–159,000) MW
Peak hourly net load	140,000 (7-year range: 127,000–140,000) MW
Average annual load	946 TWh/year
Average annual net load	755 TWh/year

Abbreviations: CSP, concentrating solar power; PV, photovoltaics.
[a]This table includes total capacity in the modeled footprint, including the Canada and Mexico portions of the Western Interconnection, although we do not consider wind deployment in these two countries.
[b]Includes cogeneration plants, biomass-fueled plants, geothermal plants, and other facilities.

TABLE 2 Turbine specifications used to generate the CF profiles for the incremental wind capacity

Technology	Land-based *current*	Land-based *future*	Offshore
Rotor diameter (m)	108	167	222
Capacity (MW)	2.1	4.5	12
Hub height (m)	80	110	136
Specific power (W/m^2)	229	205	310
Swept area (m^2)	9160	21,900	38,700
Turbine losses (%)[a]	16.7	16.7	16.7

Abbreviation: CF, capacity factor.
[a]Here, turbine losses are applied as a fixed percentage in every hour, which is a simplification. It is a combination of 15% hourly losses (accounting for array wake losses, transmission losses from substation, and blade soiling) and a 98% availability factor.[40]

and taller turbines, exhibiting a larger generator capacity, hub height, and rotor diameter.[38] Given these changes, we model a future technology to estimate whether such continued evolution will have a measurable effect on CC. For offshore turbine specifications, we assess only one set of parameters, representing a turbine that is in prototype testing (e.g., the General Electric GE220-12-MW Haliade-X) and is expected to be commercially available by 2021.[39] As of 2020, there are no commercial-scale offshore wind turbines in the Western United States so it is less clear which turbines would be deployed or how they might advance, which is why we only evaluate one technology for offshore wind sites. Finally, we note that the turbine configurations were selected to represent specific wind technology evolution but have not been optimized based on cost, CF, or CC.[39,22]

Figure 2 illustrates a histogram of the 7-year CFs of all 10,113 grid cells for both land-based technology types and offshore wind. The land-based technology configurations yield a mean CF of 25% and 28% for *current* and *future* technologies, respectively, while the offshore configuration yields a mean CF of 42%. For comparison, the annual mean CF for existing installed land-based wind capacity in the United States is 35%.[30] In this systematic analysis, we consider every grid cell (when many are obviously unrealistic for wind development), which substantially decreases the mean observed CF compared to existing wind that is largely located at favorable CF locations. The mean CF (using the *current* technology configuration) for only grid cells with existing wind deployment is much higher (33%), which is fairly consistent with existing wind in the Western United States.[38] For *future* land-based configurations, mean CFs across all sites are similar compared to the *current* land-based configuration. Projections for future turbine advances could much more dramatically increase the CF beyond the *future* configuration evaluated here.[41,29] Since this analysis uses a near-term representation of the power system (including transmission topology and renewable energy penetration), using aggressive future assumptions for wind turbine technologies would not have been realistic but will be necessary in future analysis. So although the CF change in the two land-based technologies shown in Figure 2 may not be dramatic, changes in the CF of an individual site or in the subannual CF profiles may impact CC, which is why we analyze both configurations for land-based wind. The CF of wind varies by geography as well, and the appendix (Figures A2 and A3) shows maps with the 7-year CF for both technology specifications.

As discussed, reliability-based CC assessment methods use system reliability measures such as LOLP, LOLE, or EUE to determine how an incremental generator impacts system reliability. The commonly used reliability-based methods to express CC are equivalent firm capacity (EFC), effective load carrying capability (ELCC), and equivalent conventional capacity (ECC).[42] EFC expresses the CC of the added unit under study in terms of a fictitious 100% reliable (firm) unit. ELCC expresses the CC in terms of the amount of additional load that can be added to the system when adding the new unit while maintaining the same reliability of the base case system. ECC, on the other hand, expresses the CC of the added unit in terms of a conventional unit with a specific forced outage rate (FOR). We use EUE as the probabilistic RA metric to quantify system risk, in order to capture the impact of new resources on reducing both the magnitude and duration of shortfalls. We use EFC as the CC metric to avoid the ambiguities in multiregion load growth associated with ELCC and the required choice of reference generator parameters associated with ECC. In other words, we compare the impact of the added wind capacity to a 100% reliable generator in the same location. For example, if a 100-MW wind farm reduces the EUE by 100 GWh and a 45-MW firm capacity unit also reduces the EUE by 100 GWh, the CC of the 100-MW wind farm is 45 MW or 45%. We calculate the system-wide EUE over 7 years of operations, before and after adding wind to each grid cell

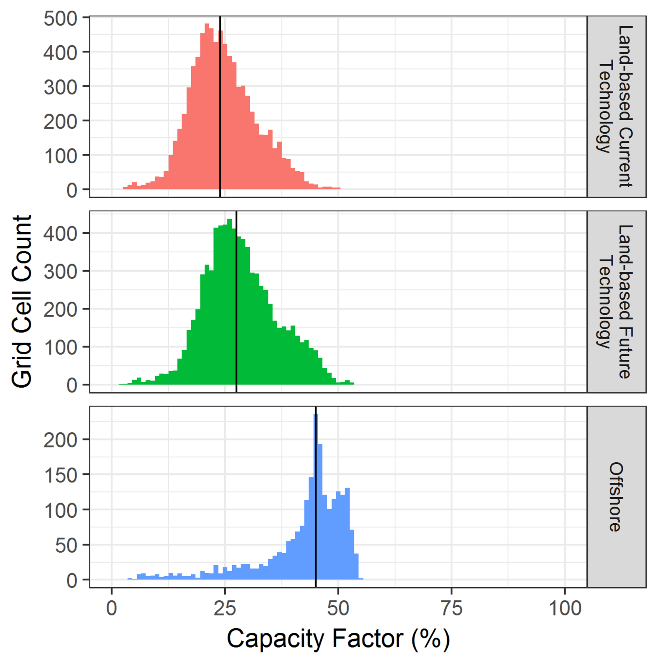

FIGURE 2 Histogram of seven-year capacity factor (CF) for both *current* and *future* land-based and offshore wind turbines. The vertical line represents the median observation

(and corresponding region). We then determine the level of firm capacity that, when added to the same region, would result in an identical reduction in system-wide EUE. The firm capacity divided by the incremental rated capacity of wind (in this case, 500 MW per cell) gives the CC.

To calculate the incremental impact of new wind resources using the EFC method, we must observe nonzero values of system LOLE and EUE to create an observable impact of marginal wind. However, our initial assessment of RA in this base case system revealed no shortfall events at all, as indicated by zero values of LOLE and EUE with 100,000 draws of random generator outages. Because many modern power systems are overbuilt, this is unsurprising.[12,15] To observe nonzero LOLE and EUE values, we must either reduce firm capacity by removing generators from the system or increase load. Our preferred solution to keep the interregional transmission consistent was to remove installed generating units with low annual CFs, as determined by an annual production cost modeling run, which amounted to 38,900 MW in total. In some regions, removing installed thermal generators with low CF did not sufficiently increase shortfall events, which resulted in the need to scale load as well (by factors between 12% and 16% depending on the weather year) until we observed nonzero EUE in all regions for each year, thus creating an observable shortfall risk to reduce with new capacity.

3 | RESULTS AND DISCUSSION

Nonzero system EUEs occur when the system is the most stressed, and generator capacity is the most essential. These times of system stress have the most influence on the CC for all generators, including wind. In this section, we first discuss these periods of system stress for this system (Section 3.1). Then we discuss the computed CC for the wind technologies (Section 3.2) and the relationship between CC and CF (Section 3.3). Finally, we examine the geographical patterns of CC in the study footprint (Section 3.4).

3.1 | Periods of system stress

Historically, many utilities (and the US Western Interconnection system as a whole) see peak demand during the late afternoon and early evening during the hot summer months. Figure 3 illustrates the average diurnal system EUEs for each month of the 7 years considered here, showing the highest levels of EUE occurring during the hot summer months, in the late afternoon or early evening. For most of the Western United States, hot summer temperatures lead to sizeable air-conditioning load that, when combined with other electricity use, results in peak electricity demand. However, not all regions of the Western US experience peak demand in the summer. Some utilities in the more temperate Pacific Northwest see peak demand in winter, highlighted by smaller and less-frequent peaks in the winter months of Figure 3. Generators that are available to produce

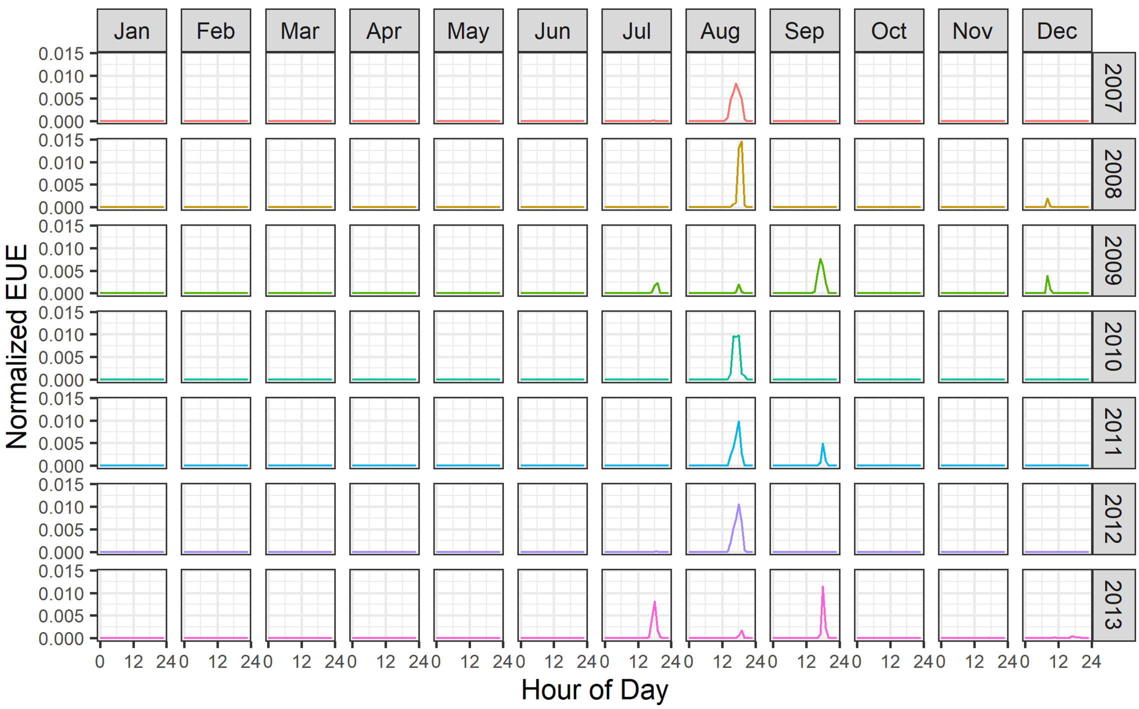

FIGURE 3 Normalized system-wide expected unserved energy (EUE) for the 7 years studied here, by month and time of day

electricity in these periods can help reduce the EUE and, thus, will exhibit higher CC. For instance, Figure 4 shows two example days in August 2007 in the Arizona Public Service (APS) territory. The top panel shows the *APS system* net load as well as the *full Western US system* EUE, shaded for emphasis. The bottom panel shows the marginal wind output of two cells in the APS area for the same 2 days. Figure 4 shows representative days as an illustration. The system EUE occurs throughout the footprint, although primarily in the Southwestern United States in this example. The availability of the wind during periods of EUE, subject to zonal transmission constraints, will determine the CC of each grid cell. Although both cells are within the APS territory, Cell4 exhibits more than three times the CC of Cell2 (36% versus 12%, respectively). Figure 4 illustrates that the generation of wind in Cell4 is much better correlated with times of nonzero EUE (shaded in the plot) than Cell2. In fact, when we weigh the hourly CF by the relative amount of EUE observed in that hour, we compute weighted CFs that are very similar to the observed CCs (38% and 12%, respectively).

3.2 | Average CC of the three wind technologies

We first present the calculated 7-year CCs for the *current* and *future* technology land-based configurations as well as offshore (Figure 5). The mean CC for *current* technology land-based wind is 16% across all sites. However, when we consider only the top quartile of sites based on CF (the 75th percentile and above), the mean CC increases to 20%. The mean CC we observe here compares to a previous analysis of the same underlying Western US system that found a wind CC between 5% and 30%, depending on the region.[20] The mean CC for the land-based *future* technology is 18%, and the mean CC for the top quartile of sites based on CF increases to 25%. So the difference between the two technology specifications is small. The slight increase in CC for the *future* technology is consistent with the increase in CF associated with the larger turbine height and diameter. Although the CFs may not change dramatically, this analysis does not consider the cost benefits larger turbines might have. In addition, we did not optimize or analyze any additional turbine specifications, and future innovation could perhaps yield turbine features that would further increase the CC of wind.

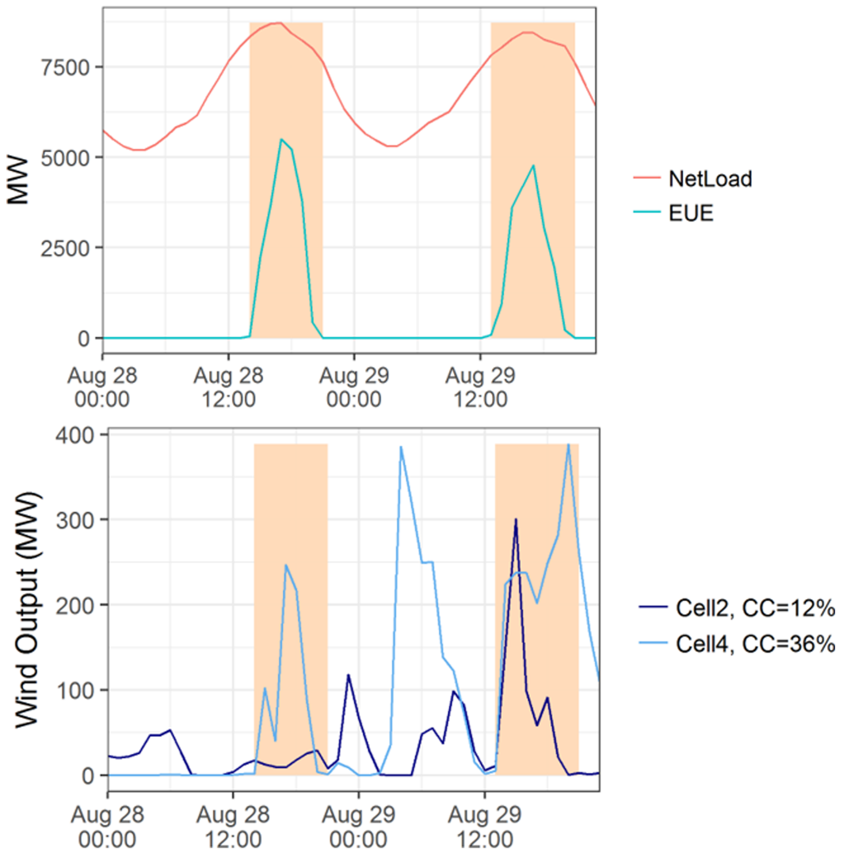

FIGURE 4 Two example days in August 2007 in Arizona Public Service (APS). The top panel shows the *APS system* net load as well as the *full Western US system* expected unserved energy (EUE), shaded for emphasis. The bottom panel shows the marginal wind output of two cells in the APS area for the same 2 days

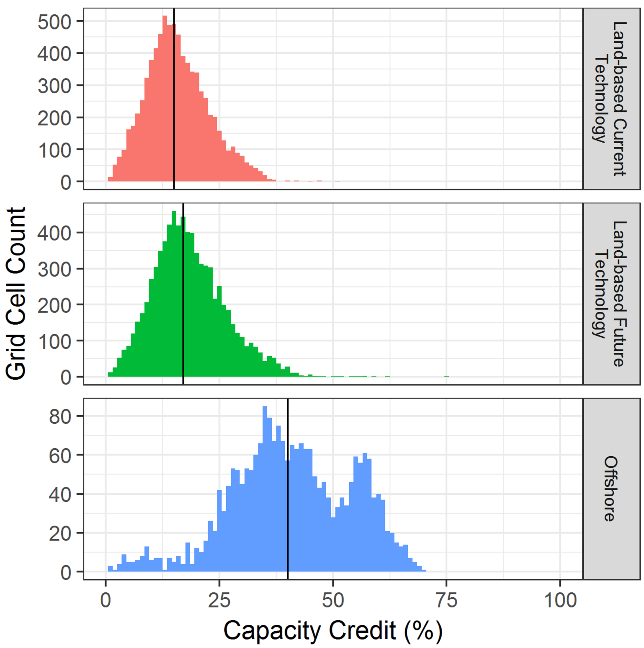

FIGURE 5 A histogram of the 7-year capacity credit (CC) calculated for the *current* technology specifications for land-based (top), *future* technology land-based (middle), and offshore (bottom) with a vertical line representing the median observation

For offshore wind, however, the mean CC is higher—41% across all sites and 53% for the top quartile of CF sites—than it is for both land-based technologies. This mean offshore CC (41%) is very close to the mean CF (42%). In contrast, the mean CC for the *current* technology for land-based wind (16%) is lower than the mean CF (25%). This implies that correlation of offshore wind patterns to times of system stress (and thus high normalized EUE) is higher than that of land-based wind. This result is consistent with previous work which shows higher CC for offshore wind compared to land-based wind, in part due to the favorable impact of the sea breeze effect for offshore generation.[43–44,13] We note that the analyzed land-based wind penetration for the footprint (8.4%) is obviously higher than offshore wind penetration (0%). If offshore wind were to grow to similar levels, we would expect the offshore wind CC to decline, although the rate of decline and how it compares with land-based wind is unclear. Future work should systematically explore how increasing wind penetration impacts CC, along with other changes to the power system.

As the histograms in Figure 5 indicate, there is a large variation in CC for wind. For example, 80% of the *current* technology land-based grid cells exhibit CCs fall between 7% and 25%. Offshore wind grid cells are more variable, with 80% of CC values falling between 27% and 60%. Several factors influence the distribution of CC between offshore and land-based wind. Firstly, we studied 2254 offshore grid cells and 7859 land-based grid cells, which means we would expect a slightly more variable histogram for offshore wind based on just the sample size. The CF histogram of offshore wind (Figure 2) also exhibits two relative peaks rather than one, which is similarly seen in the histogram for the CC of offshore wind.

3.3 | CC and CF

We also observe the relationship between CF and CC for the three wind technologies, as shown in Figure 6, which shows the CF and CC for each grid cell. Not surprisingly, the CC tends to increase with CF. This plot reinforces the conclusion that CC is generally lower than CF for land-based profiles (because most points fall below the unity line) and that the CC is similar to CF for offshore profiles (because the unity line roughly evenly divides the points). As the plot shows, the CC of offshore wind at many sites is greater than its CF, owing to a correlation of generation availability during times of system need. However, the scattered points in the plot indicate that the CF is not the only factor determining the CC of each site. More important than the 7-year average CF is the correlation of wind generation with times of system need.

3.4 | Geographical considerations for CC

Finally, we can observe geographical trends in wind CC as seen in Figure 7, which shows the CC of the *current* technology land-based sites with the offshore sites. As discussed previously, most of the highest wind CC sites are offshore. However, some land-based sites also exhibit high CCs, especially in eastern Colorado and Wyoming and in southern Arizona and New Mexico. In the case of Colorado and Wyoming, these sites have

FIGURE 6 The relationship between grid cell capacity factor (CF) and capacity credit (CC) for both land-based technologies and offshore sites, with a black slope = 1 line for reference

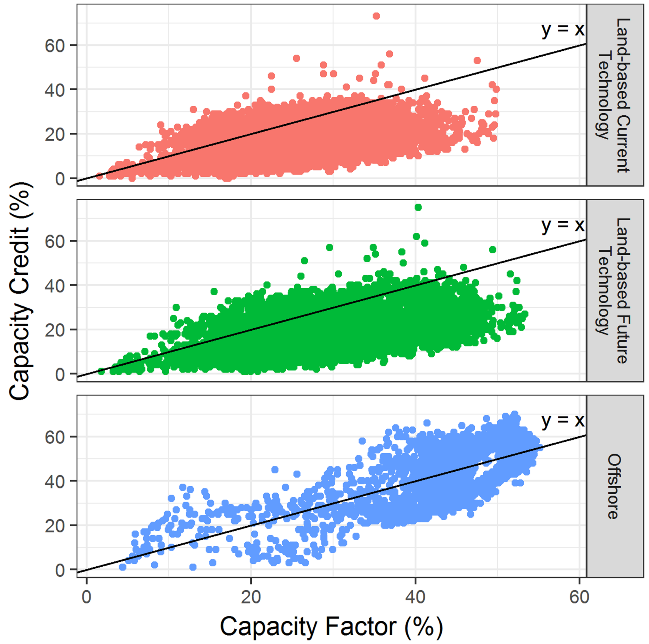

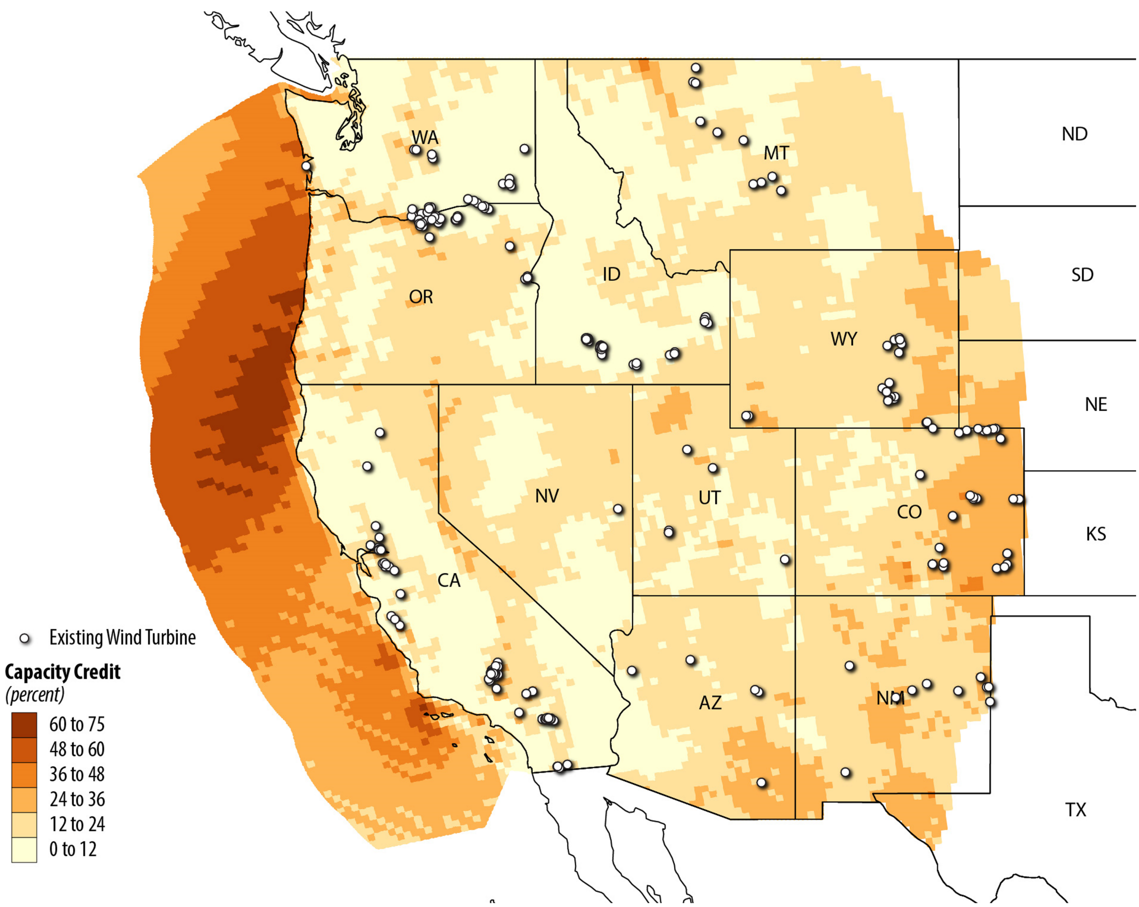

FIGURE 7 Marginal capacity credit (CC) by region for *current* land-based technology and offshore wind

higher CFs as well (appendix Figure A2). Some regions (particularly southern AZ) do not exhibit an extremely high CF, but the high CC indicates that the wind resource is well-correlated with times of system need. Appendix Figure A4 illustrates the ratio of CC to CF, indicating those regions (e.g., southern Arizona and along the southern coast in California) that exhibit this favorable correlation.

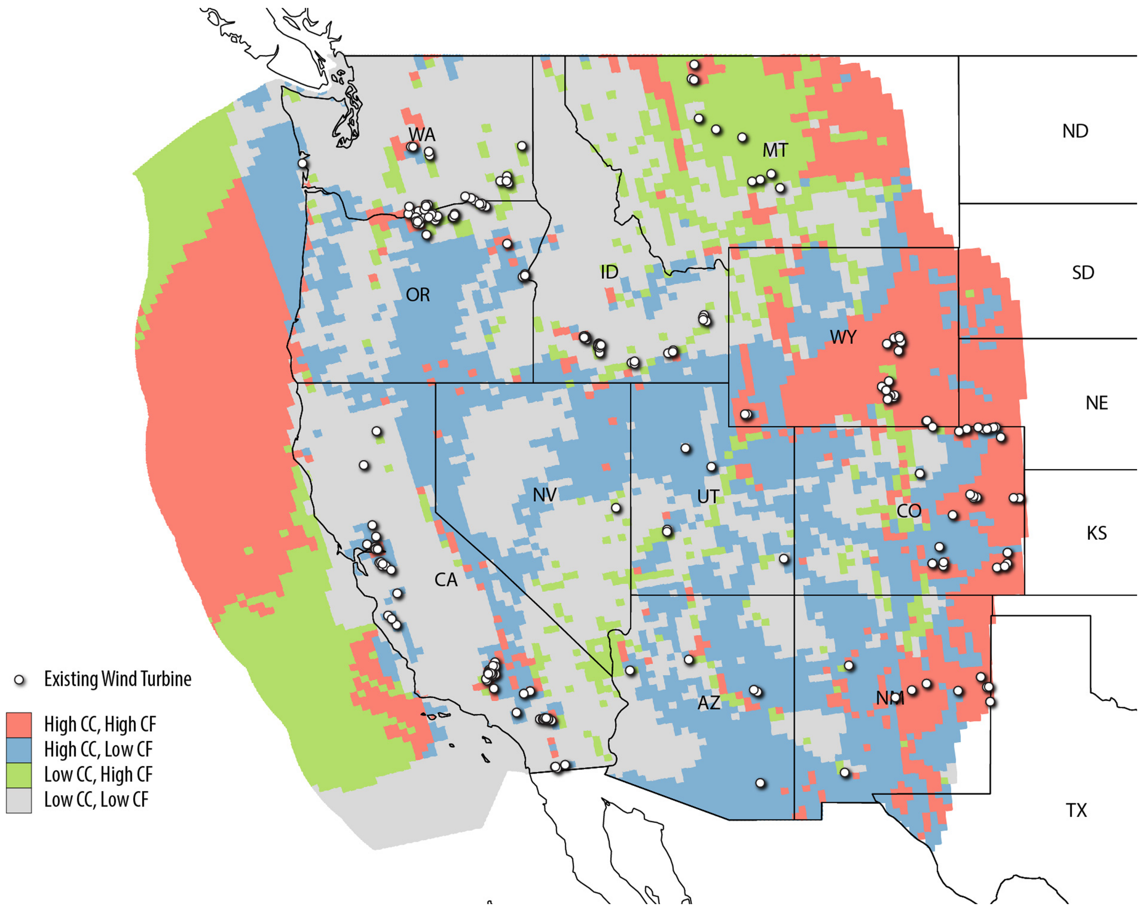

FIGURE 8 Map classifying each grid cell with high or low capacity credit (CC) and capacity factor (CF). The median CC and CF serve as the dividing point between high and low cells for offshore wind. Land-based wind likewise uses the median CC but for CF instead uses 29% (the 75th percentile) as the dividing line between high and low categorizations

However, wind CC is only one factor in determining where and when wind energy is deployed. Other important variables are the CF and energy value of wind, access to land and transmission, environmental and wildlife impact, social acceptance, and state or regional renewable energy goals. For instance, a potential wind site with high CC may be rejected because of low CF. Figure 8 classifies each grid cell into four categories: (1) High CC, High CF; (2) High CC, Low CF; (3) Low CC, High CF; and (4) Low CC, Low CF. The division between Low CC and High CC is determined by the median CC for the *current* land-based technology and offshore wind, respectively. However, the median CF for land-based wind is 24% which is lower than the actual CF of installed wind. So Figure 8 instead uses 29% (representing the top quartile, or 75th percentile and above) as the cutoff for High CF and Low CF land-based sites, using the median CF of offshore wind (45%) for offshore wind. The map shows fewer red and green cells—but still a high density of "High CC, High CF" sites in the eastern part of the footprint—as well as some scattered throughout the other western states. Grid cells with high CF and CC would be the most likely sites for potential development, whereas cells with low CC and CF would perhaps be least favorable. We observe "High CC, High CF" cells off the coast of Northern California and covering much of the eastern Rocky Mountain states. However, these "High CC, High CF" grid cells are dispersed through the rest of the western states as well, indicating possible favorable wind resources throughout. In addition, the "High CC, Low CF" or "Low CC, High CF" grid cells may still be considered for local planning entities if access to the "High CC, High CF" regions is not possible or are excluded due to land or transmission access, for instance. The difference between "High CC, Low CF" and "Low CC, High CF" cells may also be impacted by system needs. For instance, a future with high wind generation may show preference to the "High CC, Low CF" sites given the need for capacity and possibility of curtailment of wind energy. The map shows that many existing wind turbines are located on "High CC, High CF" red sites or "Low CC, High CF" green sites because high CF sites are currently prioritized for development.

4 | CONCLUSIONS

Our analysis presents a systematic evaluation of the CC of wind in the Western United States using state-of-the-art probabilistic modeling with multiple weather years. We find that wind CC varies by location but averages 16% for land-based turbines and 41% for offshore turbines, with large regional variations. Not only is the average CF higher for offshore wind (42% compared to 25% for land-based), but many offshore sites show higher CC than CF, indicating that offshore wind can be particularly well-correlated with system needs, as has been observed in the Eastern United States as well.[43] This is an important consideration since the Western US coastal states have policies that mandate expansion of renewable energy generation.[45] We also find that using *future* turbine technology (characterized by higher hub-heights and larger rotor diameters) only slightly increases the CF and CC for land-based wind but does not meaningfully change any observed geographical CC trends compared to the current turbine technology. However, the *future* technology studied here may not be reflective of advances in turbines that may take place in the following decades, and significantly larger turbines should be studied in future work.

Much of the high CC and high CF wind sites are concentrated off the northern California coast (for offshore) and in the eastern Rocky Mountain states such as Wyoming, Montana, Colorado, and New Mexico (for land-based). However, high CC and high CF wind sites are dispersed throughout the other western states as well, indicating possible favorable wind resources in nearly all Western US states. We consider only the Western United States, but given active interest in new offshore wind development in the Eastern United States, such a regional examination could help inform the potential trade-offs between offshore wind resources in the region and other resources, including importing land-based wind generation from inland.[21,46]

Finally, CC is only one consideration in the value and potential deployment of wind. Although sites identified here may exhibit high CC, they may be economically unfavorable or prohibitive because of other factors (e.g., land and transmission availability). Though a full wind deployment analysis should consider CC, many other factors that might outweigh the importance of CC would ultimately determine the location and amount of wind built. We represent the current Western US power system which has relatively low land-based wind generation (and presently **no** offshore deployment) with the intent to inform near-term planning decisions and investments. However, previous analysis has shown an important relationship between wind generation and CC, whereby existing wind deployment reduces the marginal CC of additional wind.[12,15] This relationship is particularly unclear for offshore wind, which we will explore in future analysis. Notwithstanding these scope limitations, our analysis presents the first systematic interconnection-wide evaluation of a potentially important value stream for wind using state-of-the-art probabilistic modeling with multiple weather years. This analysis can be used to inform wind plant development, energy policy, and other power system planning activities, opening up a whole new realm of research.

ACKNOWLEDGEMENTS

We would like to thank Jaquelin Cochran, Philipp Beiter, Dan Bilello, Patrick Gilman, Eric Lantz, Paul Denholm, Sinnott Murphy, Nick Grue, Anthony Lopez, and Billy Roberts for helpful input during the analysis and publication process. The research was performed using computational resources sponsored by the Department of Energy's Office of Energy Efficiency and Renewable Energy and located at the National Renewable Energy Laboratory. We gratefully acknowledge funding for this work from the US Department of Energy's Office of Energy Efficiency and Renewable Energy under contract DE-AC36-08GO28308. The views expressed in the article do not necessarily represent the views of the DOE or the US Government. The publisher, by accepting the article for publication, acknowledges that the US Government retains a nonexclusive, paid-up, irrevocable, worldwide license to publish or reproduce the published form of this work or allow others to do so, for US Government purposes.

PEER REVIEW

The peer review history for this article is available at https://publons.com/publon/10.1002/we.2620.

ORCID

Jennie Jorgenson https://orcid.org/0000-0003-2622-702X

REFERENCES

1. Billington R, Allan RN. Reliability Evaluation of Power Systems, 1984.
2. Mills A, Wiser R. Changes in the Economic Value of Variable Generation at High Penetration Levels: A Pilot Case Study of California, tech. rep., Ernest Orlando Lawrence Berkeley National Lab (LBNL), Berkeley, CA (United States), 2012.
3. Sioshansi R, Madaeni SH, Denholm P. A dynamic programming approach to estimate the capacity value of energy storage. *IEEE Trans Power Syst*. 2013;29(1):395-403.
4. Probabilistic Adequacy and Measures. Technical Reference Report Final, tech. rep., North American Electric Reliability Corporation (NERC), 2018.
5. Milligan M. A comparison and case study of capacity credit algorithms for intermittent generators, tech. rep., National Renewable Energy Lab., Golden, CO (United States), 1997.
6. Milligan M. Modelling utility-scale wind power plants. Part 2: capacity credit. *Wind Energy*. 2000;3(4):167-206.
7. Keane A, Milligan M, Dent CJ, et al. Capacity value of wind power. *IEEE Trans Power Syst*. 2010;26(2):564-572.
8. Awara S, Zareipour H, Knight A. Solar power capacity value evaluation—A review, in 2018 *IEEE Canadian Conference on Electrical & Computer Engineering (CCECE)*, pp. 1-5, IEEE, 2018.
9. Ensslin C, Milligan M, Holttinen H, O'Malley M, Keane A. Current methods to calculate capacity credit of wind power, IEA collaboration, in 2008 IEEE Power and Energy Society General Meeting-Conversion and Delivery of Electrical Energy in the 21st Century, pp. 1–3, IEEE, 2008.
10. Milligan M, Frew B, Ibanez E, Kiviluoma J, Holttinen H, Soder L. Capacity value assessments of wind power. *Wiley Interdisciplinary Rev Energy Environ*. 2017;6(1):1-15.

11. Milligan M, Porter K. Determining the capacity value of wind: An updated survey of methods and implementation, tech. rep., National Renewable Energy Lab.(NREL), Golden, CO (United States), 2008.
12. Awara S, Ardakani AJ, Zareipour H, Knight A. Assessing Capacity Value of Wind in Alberta, 2018.
13. Energy G. New England wind integration study," *Holyoke, MA: ISO New England Inc*, pp. 1–10, 2010. https://www.iso-ne.com/static-assets/documents/committees/comm_wkgrps/prtcpnts_comm/pac/mtrls/2010/nov162010/newis_iso_summary.pdf Accessed August, 24 2020.
14. Giebel G. A variance analysis of the capacity displaced by wind energy in Europe. *Wind Energy*. 2006;10:69-79.
15. Hasche B, Keane A, O'Malley M. Capacity value of wind power, calculation, and data requirements: the Irish power system case. *IEEE Trans Power Syst*. 2010;26(1):420-430.
16. Ibanez E, Daryanian B, Stenclik D. Capacity value of Canadian wind and the effects of decarbonization, in 2017 Ninth Annual IEEE Green Technologies Conference (GreenTech), pp. 59–66, IEEE, 2017.
17. Nguyen C, Ma C, Hailu A, Chalak M. Factors influencing calculation of capacity value of wind power: a case study of the Australian National Electricity Market (NEM). *Renew Energy*. 2016;90:319-328.
18. Parsons B, Milligan M, Zavadil B, et al. Grid impacts of wind power: a summary of recent studies in the United States. *Wind Energy*. 2004;7(2):87-108.
19. Tapetado P, Usaola J. Capacity credits of wind and solar generation: the Spanish case. *Renew Energy*. 2019;143:164-175.
20. Ibanez E, Milligan M. Comparing resource adequacy metrics, tech. rep., National Renewable Energy Lab.(NREL), Golden, CO (United States), 2014.
21. Beiter PC, Lau JK, Novacheck JE et al. The Potential Impact of Offshore Wind Energy on a Future Power System in the US Northeast, tech. rep., National Renewable Energy Lab.(NREL), Golden, CO (United States), 2020.
22. National Renewable Energy Laboratory. *2019 Annual Technology Baseline*, 2019.
23. Rhodes J, King C, Gulen G, et al. A geographically resolved method to estimate levelized power plant costs with environmental externalities. *Energy Policy*. 2017;102:514-515.
24. Brown A, Beiter P, Heimiller D et al. Estimating renewable energy economic potential in the united states: Methodology and initial results, tech. rep., National Renewable Energy Lab.(NREL), Golden, CO (United States), 2016.
25. Stephen G. Department of Energy Office of Energy Efficiency and Renewable Energy, "Probabilistic resource adequacy suite (PRAS)," 2019.
26. Frew B, Stephen G, Sigler D, Lau J, Jones WB, Bloom A. Evaluating resource adequacy impacts on energy market prices across wind and solar penetration levels. *Electr J*. 2019;32(8):106629, 1-8.
27. Stephen G, Hale E, Cowiestoll B. Managing solar photovoltaic integration in the western united states: Resource adequacy considerations, tech. rep., National Renewable Energy Lab.(NREL), Golden, CO (United States), 2020.
28. Hale E, Gagnon P, Jorgenson J et al. Planning for high solar photovoltaic penetrations in the western united states: Executive summary, tech. rep., National Renewable Energy Lab.(NREL), Golden, CO (United States), 2020.
29. Wiser R, Bolinger M, Hoen B, et al. *Wind Energy Technology Data Update: 2020 Edition*. Berkeley, CA (United States): Ernest Orlando Lawrence Berkeley National Lab (LBNL); 2020.
30. U.S. Energy Information Administration. ELECTRICITY Form EIA860 detailed data with previous form data (EIA-860A/860B), 2020.
31. Maclaurin G, Grue N, Lopez A, Heimiller D. The renewable energy potential (rev) model: a geospatial platform for technical potential and supply curve modeling, tech. rep., National Renewable Energy Lab.(NREL), Golden, CO (United States), 2019.
32. Cole WJ, Frazier A, Donohoo-Vallett P, Mai TT, Das P. 2018 standard scenarios report: a us electricity sector outlook, tech. rep., National Renewable Energy Lab.(NREL), Golden, CO (United States), 2018.
33. Sengupta M, Xie Y, Lopez A, Habte A, Maclaurin G, Shelby J. The national solar radiation database (NSRDB). *Renew Sustain Energy Rev*. 2018;89:51-60.
34. Draxl C, Clifton A, Hodge B-M, McCaa J. The wind integration national dataset (WIND) toolkit. *Appl Energy*. 2015;151(1):355-366.
35. Blair N, DiOrio N, Freeman J, et al. System advisor model, SAM general description (version 2017.9.5), tech. rep., National Renewable Energy Lab.(NREL), Golden, CO (United States), 2018.
36. Brinkman G, Novacheck J, Ho J et al. The Canadian Perspective on the North American Renewable Integration Study (NARIS), tech. rep., National Renewable Energy Lab.(NREL), Golden, CO (United States), 2020 forthcoming.
37. Mai T, Barrows C, Lopez A, Hale E, Dyson M, Eurek K. Implications of model structure and detail for utility planning. scenario case studies using the resource planning model, tech. rep., National Renewable Energy Lab.(NREL), Golden, CO (United States), 2015.
38. Wiser R, Bolinger M. 2018 wind technologies market report: Summary, tech. rep., Ernest Orlando Lawrence Berkeley National Lab (LBNL), Berkeley, CA (United States), 2018.
39. Musial WD, Beiter PC, Nunemaker J, Heimiller DM, Ahmann J, Busch J. Oregon offshore wind site feasibility and cost study, tech. rep., National Renewable Energy Lab.(NREL), Golden, CO (United States), 2019.
40. Stehly T, Beiter P. 2018 Cost of Wind Energy Review, tech. rep., National Renewable Energy Lab.(NREL), Golden, CO (United States), 2019.
41. International Renewable Energy Agency. *Future of Wind: Deployment, Investment, Technology, Grid Integration, and Socio-Economic Impacts*. IRENA; 2019.
42. Soder L, Amelin M. A review of different methodologies used for calculation of wind power capacity credit, in 2008 IEEE Power and Energy Society General Meeting-Conversion and Delivery of Electrical Energy in the 21st Century, pp. 1–5, IEEE, 2008.
43. Dvorak M, Corcoran B, Ten Hoeve J, McIntyre N, Jacobson M. US east coast offshore wind energy resources and their relationship to peak-time electricity demand. *Wind Energy*. 2013;16(7):977-997.
44. Energy G. The effects of integrating wind power on transmission system planning, reliability, and operations. Report on phase 2. Prepared for the New York State Energy Research and Development Authority, tech. rep., 2005.
45. Barbose G. U.S. Renewables Portfolio Standards 2019 Annual Status Update, tech. rep., Lawrence Berkeley National Laboratory, Berkeley, CA (United States), 2019.
46. Sheridan B, Baker S, Pearre N, Firesone J, Kempton W. Calculating the offshore wind power resource: robust assessment methods applied to the U.S. Atlantic coast. *Renew Energy*. 2012;43:224-233.

How to cite this article: Jorgenson J, Awara S, Stephen G, Mai T. A systematic evaluation of wind's capacity credit in the Western United States. *Wind Energy*. 2021;24:1107–1121. https://doi.org/10.1002/we.2620

APPENDIX A.

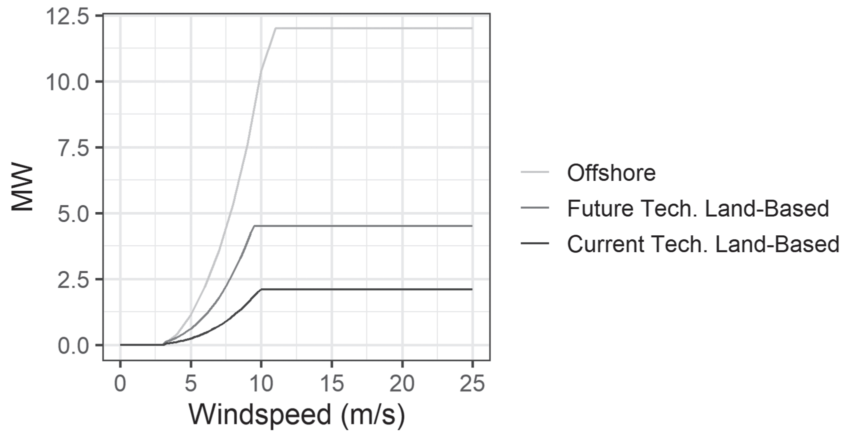

FIGURE A1 The power curves for the wind turbines evaluated

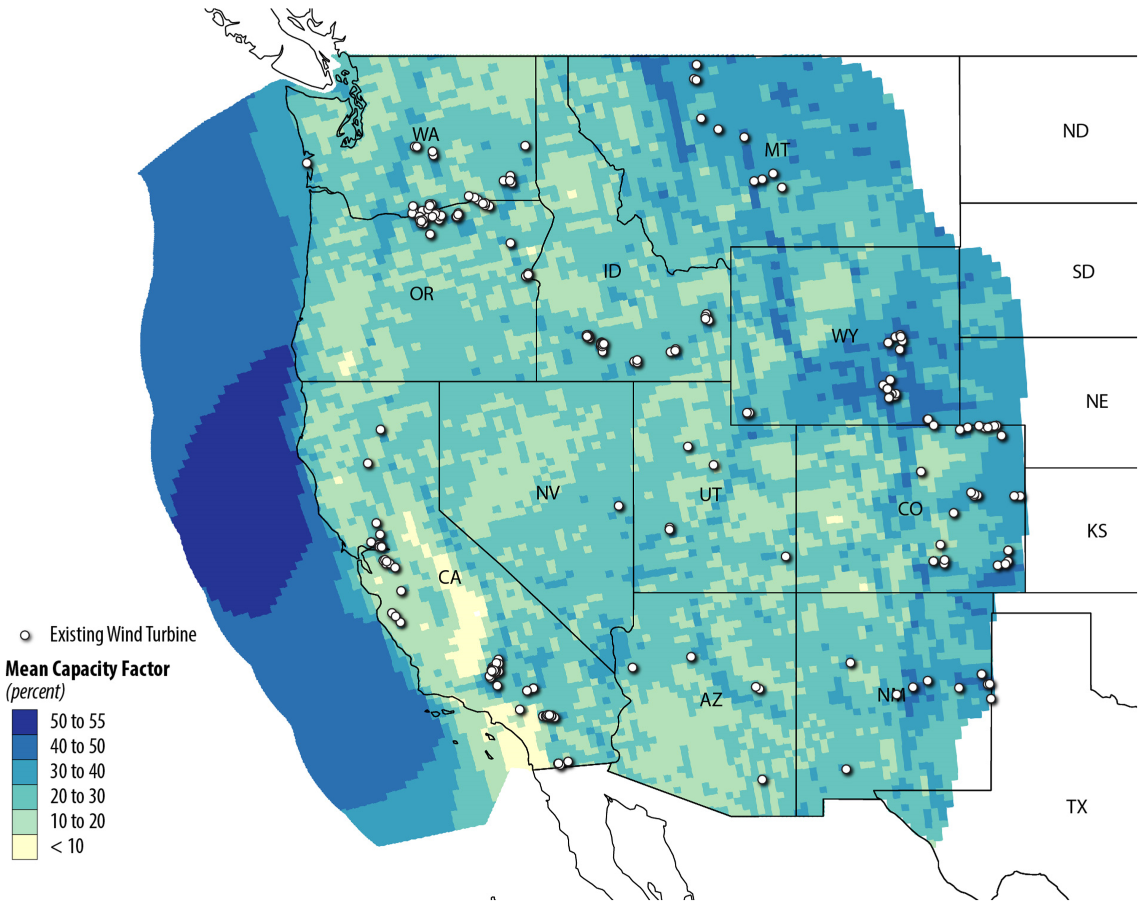

FIGURE A2 A map of the average 7-year capacity factor for each grid cell in the Western United States for the *current* land-based technology and offshore wind technologies

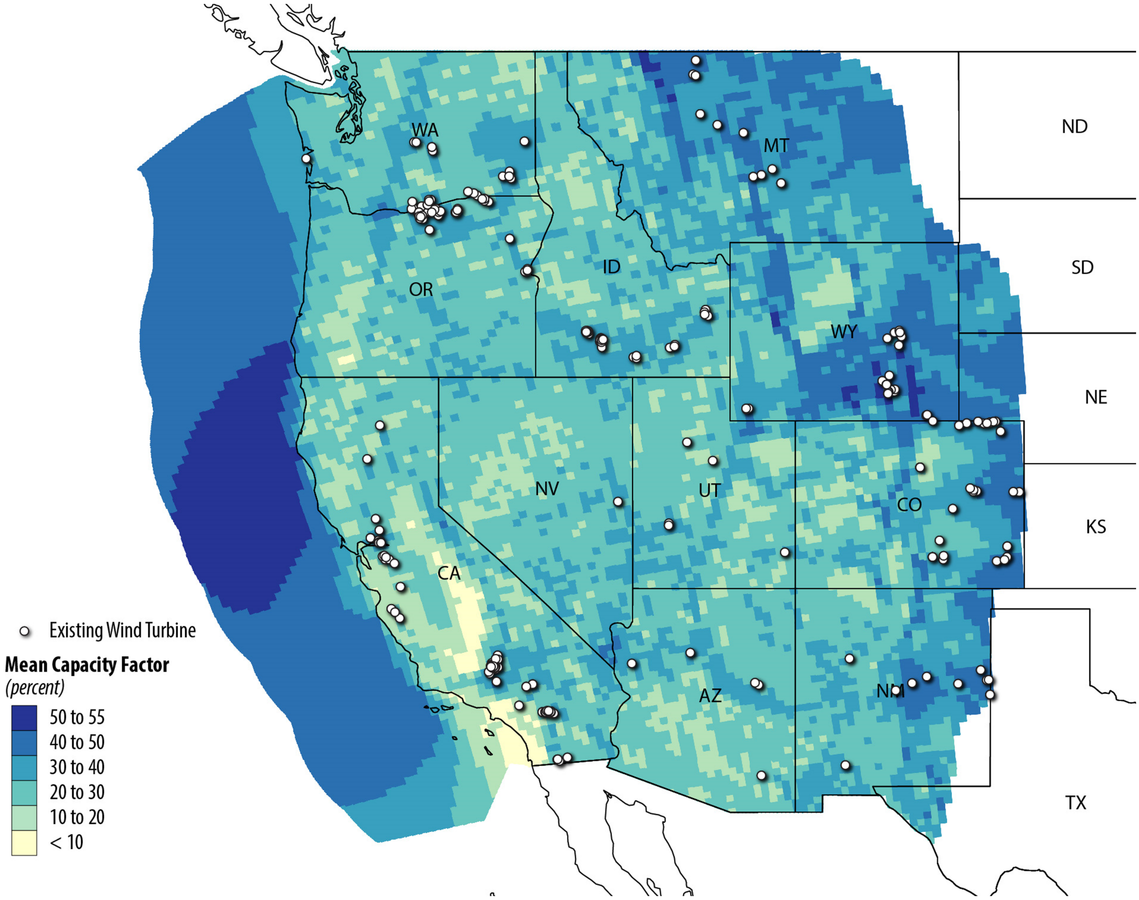

FIGURE A3 A map of the average 7-year capacity factor for each grid cell in the Western United States for the *future* land-based technology and offshore wind technologies

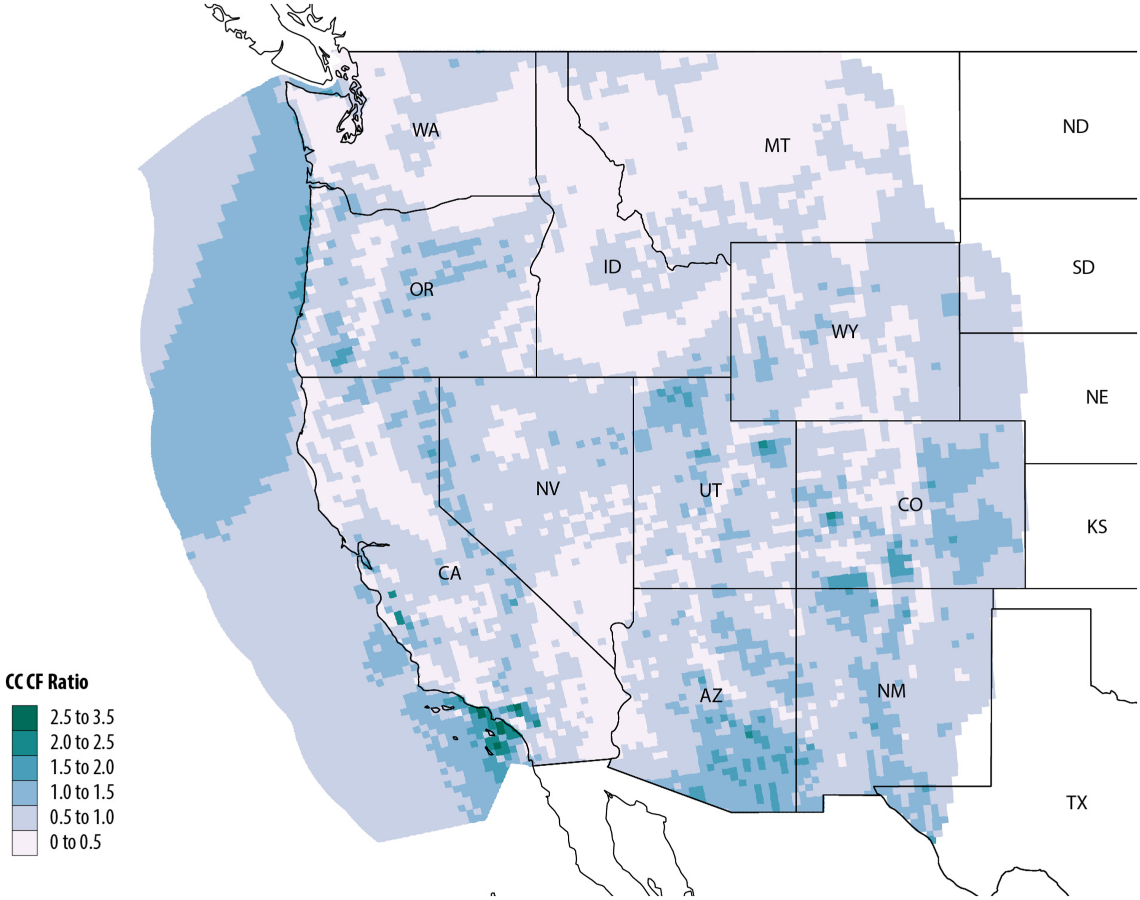

FIGURE A4 A map of the 7-year capacity credit to 7-year capacity factor mean ratio for each grid cell in the Western United States for both *current* technology land-based and offshore wind